Pergamon

PII: S0191-8141(97)00060-6

Journal of Structural Geology, Vol. 20, No. 2/3, pp. 243 to 254, 1998

0191-8141/98 $19.00 + 0.00

Use of extension testing to investigate the influence of finite strain on the rheological behaviour of marble

E. H. RUTTER

Rock Deformation Laboratory, Department of Earth Sciences, University of Manchester, Manchester M13 9PL, UK

(*Received* 20 *December* 1996; *accepted in revised form* 29 *July* 1997)

Abstract—Most mechanical testing of rocks at high temperatures is carried out under axisymmetric triaxial shortening to small (<20%) strains. However, the most significant geological deformations involve much higher strains, especially in plastic shear zones where there has been strain localization. Highly strained rocks commonly are microstructurally modified by dynamic recrystallization, so that the sheared rock is microstructurally quite different from its protolith.

High strain deformation in experiments can be induced by direct shear or through torsion, or by taking advantage of the tendency for extensional deformations to result in necking. It is important to be able to separate out the geometrical factors favouring localization from those arising from strain-dependent microstructural changes. Here, we present the results of high strain (>1000%) axisymmetric extension tests on Carrara marble at 700°C and 800°C, in the form of strain–time plots for the evolution of material sections through the sample at different distances from the neck. At 800°C, it is clear that total dynamic recrystallization by grain boundary migration is accompanied by substantial mechanical weakening, but sufficient strain could not be applied to reach the steady-state condition for the recrystallized material. The recrystallization is interpreted to produce weakening because the migration of grain boundaries sweeps grains clear of accumulating dislocation density faster than recovery by dislocation climb. In nature, such mechanical weakening would be expected to favour the stable development of a localized zone of deformation. © 1998 Elsevier Science Ltd.

INTRODUCTION

Most of what we know of the rheology of rocks at high temperatures has been obtained from axisymmetric shortening experiments on rock cylinders. Such tests normally only provide reliable stress data up to perhaps 25% shortening, beyond which the specimen becomes progressively inhomogeneously deformed. Specimens shortened to 50% or more usually only provide microstructural and fabric information (Drury *et al.*, 1985; Rutter *et al.*, 1994).

A great deal of rheological modelling of the lithosphere has been carried out assuming that rock flow is in a steady state (flow at constant strain rate, constant stress, constant temperature and at constant microstructure). It is clear, however, that plastic flow of rocks commonly involves progressive development of grain shape fabric, formation of crystallographic preferred orientation, and dynamic recrystallization with or without grain size change. All these microstructural changes can, in principle, lead to strain-dependent changes in flow stress. Mechanical weakening with increasing strain is likely to lead to localization of flow, for example into shear zones, natural examples of which frequently show extreme microstructure and fabric changes relative to the protolith. Given the geologically perceived importance of shear zones in the accommodation of large lithospheric displacements, it is the mechanical behaviour of such highly strained rocks that is likely to affect most strongly the effective rheology of the lithosphere.

A number of possible approaches can be taken to discover the strain dependence of the flow behaviour of rocks. These include the testing of naturally occurring rocks that had previously been strained by varying amounts, potentially samples taken from across the margin of a natural shear zone. Alternatively, high-temperature testing in torsion can allow very large (rotational) shear strains to be accumulated. The potential of both these approaches has yet to be explored (but see Casey *et al.* (1998)). Schmid *et al.* (1987) have successfully produced large strains in marble in direct shear at high temperatures by embedding a sample in the form of a thin slice inclined at 35° to the loading axis in a sawcut cylinder of non-deformable material.

The approach explored here uses axisymmetric extension testing under confining pressure to access large (irrotational) strains when the deformation involves the formation of a localized neck. Extensional deformation in the neck can exceed 1000%. High-temperature extension testing has been used several times previously in studies of the steady-state (low-strain) rheology of marble (Heard, 1963; Heard and Raleigh, 1972) and halite (Carter and Heard, 1970), but its full potential for rocks seems not to have been explored. In contrast, extension testing under unconfined conditions has long been used in the study of the mechanical behaviour of metals. In this paper, extension tests are reported on Carrara marble deformed at 700°C and 800°C, at a constant bulk extension rate. Under these deformation conditions, the rock undergoes total dynamic recrystallization at high strains (Fig. 1). From these tests, the effect of strain on the flow stress has been investigated.

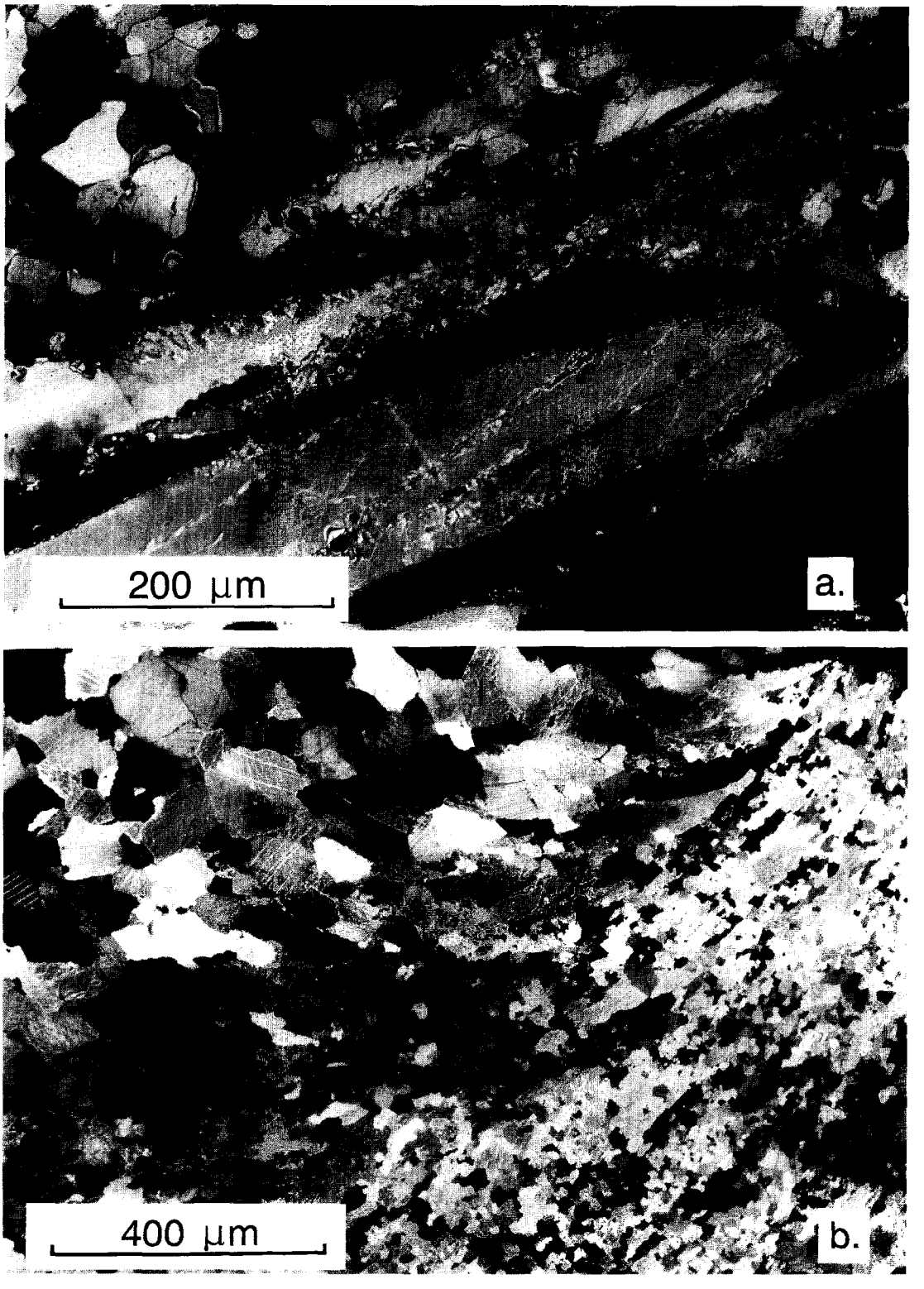

Fig. 1. Optical photomicrographs (crossed polars) of Carrara marble experimentally deformed at (a) 300 MPa and (b) 200 MPa confining pressure. (a) Necked region of specimen extended at 700°C, showing the recrystallization sequence. The large, highly elongate (about × 10 extension) old grains show initial recrystallization in the grain boundary regions by grain boundary bulging and subgrain rotation. These provide nuclei for the eventual total recrystallization of the specimen by grain boundary migration to produce larger, strain-free grains such as those visible at top left and extreme right. (b) Corner of specimen shortened vertically by 40% at 800°C. The loading piston was in contact with the top edge of the specimen. Thus the top left of the field of view is unstrained due to the 'pressure shadow' effect of the rigid piston. The area bottom right is highly strained and has begun to flow around the corner of the loading piston (top right). The strained area, and the whole of the central region of the sample, has totally recrystallized by grain boundary migration to an aggregate of smaller, strain-free, equant grains with an intense crystallographic preferred orientation. The grain size reduction is insufficient to move the deformation mechanism into the grain-size-sensitive deformation mechanism field.

COMPARISON OF EXTENSIONAL WITH CONTRACTIONAL TESTING ON ROCKS UNDER CONFINING PRESSURE

Figure 2 shows the comparative appearance of rock samples deformed by large amounts in axisymmetric shortening (contraction) and extension. When the deformation is carried out at high temperature under confining pressure, a thin-walled metal jacket must be sealed to the loading pistons to prevent ingress of the confining medium (usually a liquid or gas). This results in a large frictional traction between the ends of the sample and the loading piston, and hence to a no-slip condition at that interface. In both cases, the sample deforms heterogeneously as a result of the no-slip condition at the specimen ends. In the deformation of ductile metals under unconfined conditions, the loading platens can be made larger than the specimen diameter. Thus, by inserting a thin lubricating layer between platens and specimen ends, slip can be permitted, which tends to ensure more homogeneous deformation up to large strains.

Compressed rock samples

The compressed rock sample develops barrelling and a conical zone of almost zero strain adjacent to each loading piston. Thus, high shear strain zones develop between these conical regions and the central part of the sample, and, at large total shortening, these are usually the first areas to undergo radical microstructural readjustment by dynamic recrystallization (Rutter, 1995). At extreme shortenings, the end regions of the sample may flow around the corners of the loading pistons. These heterogeneities begin after about 20–25% bulk shortening. Data-processing to produce a stress–strain curve is usually carried out under the assumption of homogeneous strain at constant volume, in order to compute the cross-sectional area increase with bulk shortening. Thus, at high strains, the stress–strain curve obtained may not represent adequately the flow behaviour of the material. Shortening tests are also usually carried out under constant displacement rate, so that the true strain rate is not constant but increases with strain. This can affect the apparent rheology when the flow is nearly linear-viscous in character, and can affect the shape of the stress–strain curve, producing apparent strain hardening at low strains. Figure 3 shows typical constant displacement rate stress–strain curves for extremely shortened Carrara marble samples processed in this way. There is apparent strain softening at high strains, but this may be a reflection of the concentration of strain into the corner shear zones, in which total dynamic recrystallization has occurred (see photomicrographs in Rutter, 1995). The strain concentration necessarily occurs for geometric reasons, but, as a result, it is not clear whether strain localization is also accompanied by any change in the intrinsic mechanical properties of the material.

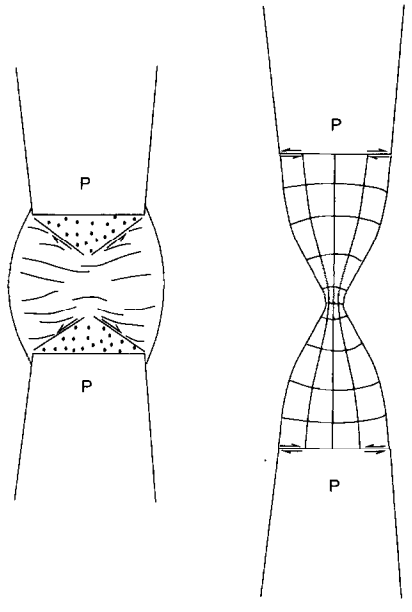

Fig. 2. Sketches to show the comparative behaviour of rocks tested under unconfined conditions in compression and in extension. The development of specimen shape in compression is strongly influenced by the no-slip condition at the interface between the specimen ends and the loading pistons. Conical zones of low strain develop at the specimen ends, and force high shear strain zones to develop as specimen material is pushed around the ends of the loading pistons. A necking instability develops in the extended sample, and strain heterogeneities across the sample at any point are less severe, hence the high strain geometry can be analysed. End conditions are less important for the behaviour of the specimen as a whole and especially in the neck. The orthogonal grid illustrates the form of the principal stress trajectories in the extended specimen.

Extended rock samples

The extended sample also develops a geometric instability that leads to localization of a neck. However, in contrast to the end regions of the shortened sample, nowhere along the length of the necked sample is there a comparable degree of strain variation across the diameter of the specimen. At any cross-section, the finite strain is given by the ratio of the initial cross-sectional area to the instantaneous area, assuming constant volume deformation. During the course of the extension, the load is the same at every cross-section, so the local stress supported varies directly with the area change. Thus, from a series of such specimens deformed to different bulk extensions, the evolution of stress and finite strain can, in principle, be determined up to large natural (true, or logarithmic) strains ($\varepsilon_3 > 2.4$, or $> 1000\%$ extension, where ε_3 is extensional logarithmic strain, $\ln(1+e_3)$, and e_3 is extensional conventional strain).

During deformation in compression, the increase of differential stress causes the mean stress on the sample to increase by an amount equal to a third of the instantaneous differential stress. In extension, the axial stress, which initially has the same value as the confining pressure, is reduced by withdrawing the loading piston,

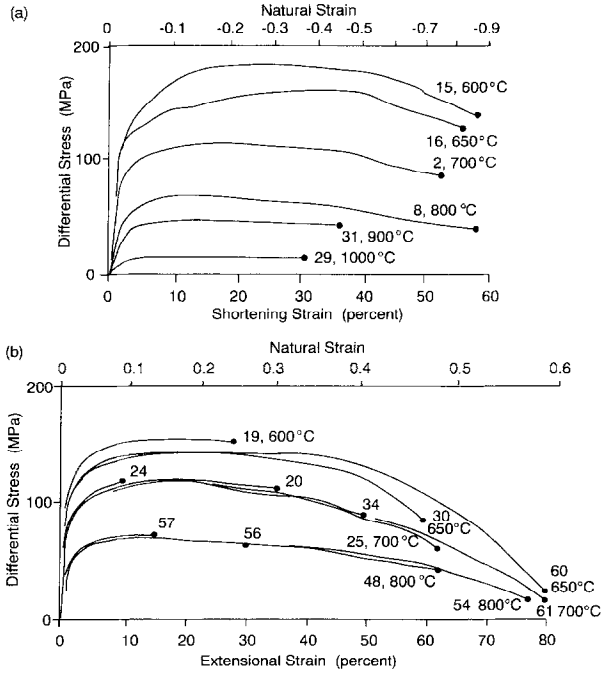

Fig. 3. Comparison of the form of stress vs bulk strain curves for Carrara marble samples (numbered) tested in axisymmetric extension and shortening at about 250 MPa mean pressure and a constant displacement rate corresponding initially to a strain rate of $\pm 8 \times 10^{-4}\,s^{-1}$. All data were processed on the assumption of homogeneous strain, an assumption progressively more seriously violated at higher bulk strains. The shapes of the curves are probably meaningful up to perhaps 30% strain. The apparent strain softening in extension reflects the necking instability, and in compression, the formation of shear zones near the specimen ends. In extension, some of the succession of stress–strain curves to progressively higher bulk strains at 700°C and 800°C are shown.

so the mean stress decreases by the same amount. During extension, therefore, all the principal stresses are compressive, and must remain so. Unlike the true tensile test, there is no need to grip the specimen ends. If the axial differential stress becomes equal to the confining pressure, there will be no resultant force pushing the specimen ends against the piston faces. Any attempt to increase the differential stress beyond that amount will cause separation of the specimen from one piston, with consequent intrusion of the metal jacket. Thus, the extension-testing technique can only be used for materials that will flow under differential stresses sufficiently smaller than the applied confining pressure that the specimen remains in the field of ductile behaviour. This restricts its use to high-temperature plastic flow of low porosity materials, or to the low-temperature deformation of intrinsically weak materials such as soils and porous rocks.

THEORETICAL ASPECTS OF THE EXTENSION TEST

The analysis of the tensile test usually follows the approach of Hart (1967), and relevant features are outlined here. Suppose that at any instant in the history of an axisymmetric extension test on a cylindrical specimen, the differential axial load is P at distance x along the sample and the differential stress is σ. At this point, the cross-sectional area is A, the natural strain is ε and the strain rate is $\dot{\varepsilon}$. Because all circular cross-sections of the specimen must bear the same load,

$$P = \sigma(x)A(x) \tag{1}$$

and

$$\frac{dP}{dx} = 0 = A = \left[\left(\frac{\partial\sigma}{\partial\varepsilon}\right)_{\dot{\varepsilon}} \frac{\partial\varepsilon}{\partial x} + \left(\frac{\partial\sigma}{\partial\dot{\varepsilon}}\right)_{\varepsilon} \frac{\partial\dot{\varepsilon}}{\partial x}\right] + \sigma\frac{dA}{dx}. \tag{2}$$

Assuming the volume of the specimen to remain constant during deformation

$$\varepsilon = \ln[A_0/A(x)] \tag{3}$$

in which A_0 is the cross-sectional area before deformation. Thus,

$$\frac{d\varepsilon}{dx} = \frac{-1}{A}\frac{dA}{dx} \tag{4}$$

and

$$\dot{\varepsilon} = -\dot{A}(x)/A(x)$$

and

$$\frac{d\dot{\varepsilon}}{dx} = -\frac{1}{A}\frac{d\dot{A}}{dx} + \frac{\dot{A}}{A^2}\frac{dA}{dx}. \tag{5}$$

Combining equations (4) and (5) into equation (2) gives

$$\frac{dA}{dx}\{\sigma - m\sigma - g\sigma\} = -\frac{d\dot{A}}{dx}\frac{m\sigma A}{\dot{A}} \tag{6}$$

or

$$(\mathrm{d}\ln\dot{A}/\mathrm{d}\ln A) = (m + g - 1)/m \tag{7}$$

in which

$$g = \frac{1}{\sigma}\left(\frac{\partial\sigma}{\partial\varepsilon}\right)_{\dot{\varepsilon}} \tag{8}$$

and

$$m = \frac{\dot{\varepsilon}}{\sigma}\left(\frac{\partial\sigma}{\partial\dot{\varepsilon}}\right)_{\varepsilon} = \left(\frac{\partial\ln\sigma}{\partial\ln\dot{\varepsilon}}\right)_{\varepsilon}. \tag{9}$$

g is a material parameter that describes the rate of strain hardening (or softening), and m measures the strain rate sensitivity of the flow stress. In the geological literature, it has been usual to express the relationship between strain rate and flow stress as $\dot{\varepsilon} \propto \sigma^n$, from which it follows that $n = 1/m$. It has been common practice in the materials literature (e.g. Hutchinson and Neale, 1977; Hu and Daehn, 1996) to describe the effect of strain and strain rate on the flow stress using a power law of the form

$$\sigma = k\varepsilon^r\dot{\varepsilon}^m \tag{10}$$

in which r is called the strain hardening exponent and k contains geometric and temperature-dependent terms. Thus,

$$r = (\mathrm{d} \ln \sigma / \mathrm{d} \ln \varepsilon)_{\dot{\varepsilon}};$$

hence, by comparison with equation (7)

$$g = r/\varepsilon. \tag{11}$$

The no-slip condition at the specimen ends causes a minimum diameter to develop in the centre of the specimen, even during the initial elastic deformation. The deformation will be non-uniform if this smallest cross-section shrinks faster than the rest. Reduction of the cross-section causes stress to rise and for the local strain rate correspondingly to increase. Provided that the strength of the material rises by a sufficient amount (by strain rate hardening or strain hardening) to compensate, the deformation will remain stable, and neck formation will not accelerate. Otherwise, the deformation continues to accelerate, or the applied load falls until separation of the specimen occurs in the neck. Intuitively, small values for m and g will favour shrinkage to form a neck. Geometrically, deformation is unstable when the rate of change of cross-sectional area accelerates, i.e.

$$\mathrm{d}\dot{A}/\mathrm{d}A > 0.$$

In extension, because the area decreases ($\dot{A}/A$ is negative), unstable deformation requires

$$(\mathrm{d} \ln \dot{A}/\mathrm{d} \ln A) < 0$$

Thus, from equation (7),

$$g + m < 1 \tag{12}$$

provides a criterion for the onset of a necking instability. For a marble at 700°C or 800°C, m is expected to be 0.2 or less (Schmid *et al.*, 1980). If flow occurs at steady state, $g = 0$, and therefore, extensional flow is always expected to be unstable. Strain-softening exacerbates the necking instability. However, even if there is a moderate strain hardening, the low m value favours instability, and therefore, the mere observation of necking instability in mechanical tests on marble tells us nothing about how the evolution of microstructure with progressive strain is affecting the rheological behaviour. It will be necessary to examine more closely the evolution of stress and strain along the length of a progressively necking specimen in order to determine whether there is a microstructural contribution towards the development of the instability.

At this point, it may be noted that superplastic flow in materials is characterized by the lack of (rapid) development of a necking instability. Extensional strains > 500% may occur without significant necking. Such flows have been observed experimentally in ultrafine-grained calcite rocks (Schmid *et al.*, 1977; Walker *et al.*, 1990; Rutter *et al.*, 1994) and are characterized by $0.5 < m < 1$ and zero rate of strain hardening (slightly positive if grain-growth occurs). From equation (12), no instability is expected when $m = 1$, but empirically, it is found for many materials that provided that $m > 0.5$, the rate of any neck growth is negligibly small. Rutter *et al.* (1994) demonstrated that for marbles characterized by $m < 0.2$, rapid neck growth occurs in extension, whereas specimens of ultrafine-grained calcite rocks extended without necking.

SAMPLE MATERIALS, APPARATUS AND EXPERIMENTAL PROCEDURE

The experiments were carried out on oven-dried cylindrical samples of white Carrara marble, 10 mm in diameter and 20 mm long, cored from the same block and in the same direction as the samples described in Rutter *et al.* (1994) and Rutter (1995). The marble has a uniform, almost equigranular microstructure, with a mean planar grain size of 130 ± 29 μm (1 standard deviation of the measured mean) determined by the linear intercept method (no stereological corrections applied) and no preferred crystallographic orientation. The trace element chemistry of these samples is given in Rutter (1995).

All of the experiments reported here were performed on an internally heated, argon gas pressure medium testing machine (Paterson Instruments). This was modified for extension testing by the incorporation of a bayonet connector between the bottom loading piston and the top of the internal axial load cell. All extension tests were run at a confining pressure of 300 MPa and at an axial displacement rate of -6.67×10^{-3} mm s^{-1}, corresponding to a nominal initial strain rate of -3.3×10^{-4} s^{-1}. Tests were performed both at 700°C and at 800°C, because it was known that complete dynamic recrystallization of the specimen would occur after strains on the order of 40% and 25%, respectively, under these conditions. For the 700°C tests, samples were jacketed in a 0.4-mm wall thickness copper jacket and for 800°C in a similar iron jacket. At temperatures above 700°C, the higher thermal conductivity of copper requires excessive furnace power dissipation. All experimental data were corrected for the load supported by the jacketing material. Differential stresses are believed to be correct to about 1 MPa after correction for jacket strength.

Temperatures are believed to be accurate to ± 5°C, and along-sample variations are within 7°C over 40 mm length (based on temperature-profiling along a hollow sample) at the start of each test. It is possible that the change in sample geometry during straining disturbs the thermal profile, and that the lower half of the sample is progressively being pulled out of the hot zone. However, uniformity of the sample necking profile was taken as an indication of an acceptably small thermal gradient along the sample at the end of a high-strain test. Four specimens whose neck was significantly off-centre were rejected. The ends of the specimen were separated from the loading pistons by recrystallized alumina discs, each

3 mm thick. During each test, specimen temperature was measured at the top (the stationary end) of the sample by means of a thermocouple introduced into contact with the top of the upper alumina disc along the hollow upper loading piston. A hollow alumina disc at the top of the specimen would cause substantial extrusion of the sample through the hole. Thus, the specimen pores were not vented to atmospheric pressure. However, any build-up of gas pressure in the specimen pores would cause separation of the components of the specimen assembly, which did not happen.

At each test temperature, a series of specimens were stretched to a succession of progressively higher bulk extensions, up to almost twice the original length. From the measured load at the end of each test and the measured cross-sectional area at different points along the length of each specimen, the variation of differential stress with length along the specimen could be calculated. Several specimens were cut longitudinally for thin-section observations of microstructure and recrystallized grain sizes, and these results have been reported in Rutter (1995).

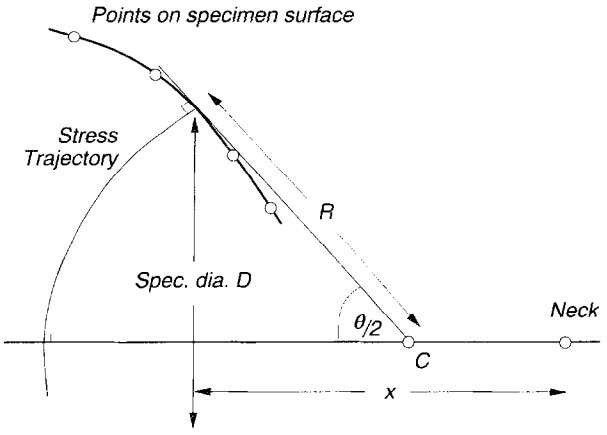

Fig. 4. Method of obtaining the axial stress at each point x (measured from the neck centre) along the deformed specimen. The stress is the final measured load divided by the area of the σ_1 stress trajectory surface, here assumed to be the zone of the sphere centred at C on the specimen axis and truncated by the specimen surface. The specimen shape was described by a series of overlapping cubic polynomial curves passing through groups of four adjacent measured diameters, so that tangent lines could be found by differentiation.

MECHANICAL DATA AND ANALYSIS OF SPECIMEN SHAPE

The shapes of the stress–strain curves obtained from the 700°C and 800°C extension tests taken to progressively higher strains are shown in Fig. 3. The bulk extensions to which each sample was taken are shown here. The raw force vs displacement data were processed in the standard way, assuming homogeneous deformation at constant volume. The apparent strain weakening is therefore partly or wholly a purely geometric result of the stress drop consequent upon the large cross-sectional area reduction in the neck. It is not clear from these stress–strain curves whether part of the stress drop is caused by, or associated with, the total dynamic recrystallization of the samples.

At each point along the shape profile, the stress, finite strain and strain rate are different. Our aim is to discover the evolution of stress, strain and strain rate at each of a succession of arbitrarily chosen points originally at 0, 0.5, 1.0, 2.0, 4.0, 6.0 and 9.0 mm from the point on the initial sample that eventually becomes the neck.

At both 700°C and 800°C, all highly stretched samples developed a marked necking instability at high bulk strains, so that true stretching strains in the centre of a specimen could exceed 2.4 (1000% extension). The shape of each specimen was described by measuring the diameter at a succession of points along the length. Cubic polynomials were fitted to a succession of overlapping groups of four points so that tangents to the profile could be obtained by differentiation. Figure 2 shows the expected form of the pattern of stress trajectories within the extended specimens. At the free surface, the trajectories must be parallel and perpendicular to the surface. In the absence of any additional information, it was assumed that the maximum principal stress trajectories would form truncated spherical surfaces. Thus, the stress acting normal to any one of these surfaces at the end of an experiment and prior to offloading would be given by the axial differential force supported (recorded by the internal load cell) divided by the area of the zone of the sphere truncated by the surface of the specimen. The geometry is shown in Fig. 4. At position x along the specimen, the diameter D is measured and the centre C on the specimen axis, and hence the radius R, of the stress trajectory sphere zone is found by extrapolation of the tangent to the specimen surface at x. If the angle subtended by the tangent cone is θ, $R = D/(2 \sin \theta/2)$, and the area A of the zone surface is given by

$$A = 2\pi R^2 \sin \theta/2(1 - \cos \theta/2).$$

In order to find the final positions of a succession of points that were initially at specified positions with respect to the neck, we assume that the deformation is isovolumetric. Thus, by treating the necked specimen as a series of frustums of circular cones of varying apical angles θ and of infinitesimal height dx, and having segmented the specimen into sections whose shape is described by cubic polynomials, it is possible to find by integration the volume of the specimen bounded by any two distances x_1 and x_2, and hence to locate the final positions along the specimen of any points of specified initial positions. A computer program was written to carry out these operations and to report for each specimen the final stress and strain values at each of the specified initial positions given above. Figure 5 shows profiles of differential stress values at the end of a succession of tests at 700°C and 800°C, corresponding to the positions of the above designated points along the

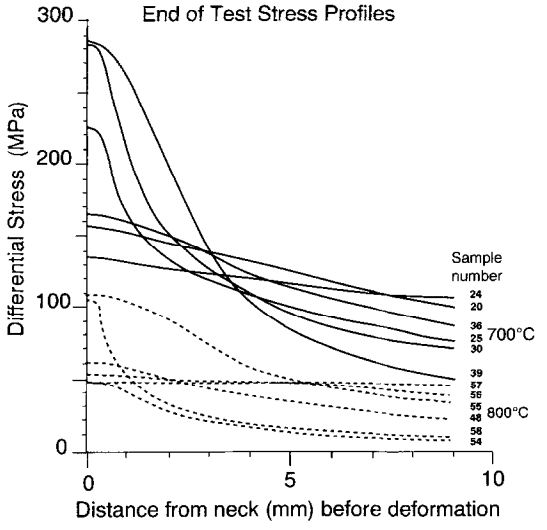

Fig. 5. Examples of calculated axial stress profiles along specimens at the end of each test (specimen number shown with each curve, compare with Fig. 6 for corresponding strain values), expressed in terms of distances before deformation from the position that will become the neck. The greatest stress intensifications in the necks correspond to greatest degrees of necking.

specimen at the beginning of each experiment. Data processed in this way for 10 specimens deformed at 700°C and seven specimens deformed at 800°C are presented in Fig. 6, as graphs of finite natural strain vs time. All specimens were deformed at the same rate of extension, and therefore, provided that behaviour is reproducible, the succession of specimens allows a history of stress and strain at specific material points along a specimen to be followed.

DESCRIPTION AND INTERPRETATION OF EXPERIMENTAL RESULTS

In Fig. 6, the finite strain at each specified point along each specimen is linked by straight lines, and the stress along each sample is shown in Fig. 7. If specimen behaviour was perfectly reproducible, these lines would link points on smooth curves. The greatest source of measurement error is in the diameter of the neck. This is squared in the calculation of strain and stress, but even in the neck, these calculated values are likely to be correct to $\pm 5\%$. The irregularities observed are therefore due mainly to irreproducible necking behaviour rather than to measurement errors. Given the small m value for this rock, the eventual neck shape evolution may be very sensitive to the precise shape developed in the elastic and immediately post-yield regimes. The effect of these geometric fluctuations is severe because when necking has been intense, so that large stresses and strains are recorded in the neck, there is a corresponding reduction of stress and strain towards the ends of the specimens. Specimen 58 in Fig. 6 shows this effect well.

In Fig. 7, manual smoothing of the material-point history curves has been attempted, and the stress values (taken from Fig. 5) have been contoured. A number of points are apparent. At any instant, the slope of a material-point history curve (bold line) is the strain rate at that instant, and strain rates become less with greater distance from the specimen centre. At 700°C, in particular, there is a marked acceleration of strain rate in the centre of the specimen after a natural strain of about 0.6. This corresponds to an acceleration of the necking instability. The acceleration is less marked at 800°C.

The way that the material-point curves intersect the stress contours should be noted. Associated with the initial yielding of the specimen, all material-point curves intersect the progressively higher stress contours. This tends to be followed by a period in which both sets of curves are parallel, corresponding to steady-state flow. This is best seen in the 700°C data away from the specimen centre where strain rates are lower. In the centre of the specimen, however, the material point curves always seem to cut the stress contours in the direction of increasing stress. This is not, however, the same as saying that the material displays a strain-hardening characteristic, for the observed stress increase is also accompanied by an increase in strain rate. A strain hardening ($g > 0$) (or softening, $g < 0$) characteristic requires hardening (or softening) to be observed at a true constant strain rate. At 800°C, it appears that, within experimental uncertainty, a steady state is maintained up to high true strains (*ca* 2.4) in the specimen centre.

At 800°C, the material-points between the neck and the specimen ends follow reasonable approximations to a true constant strain rate (Fig. 7). However, it is unequivocally clear that these material-point curves intersect the stress contours in the direction of decreasing stress, indicating that real strain softening is occurring. The effect is less clear at 700°C, because the downcutting also appears to be accompanied by a flattening of the material-point curves, indicative of a decrease in strain rate that could account for the apparent weakening.

An approximation to true constant strain rate curves can be made on these figures, by constructing isoclines to the material-point curves. An example is shown in Fig. 7 for 700°C and should be considered as an approximation to the true constant strain rate response for a range of strains, strain rates and stresses because the isocline does not correspond to one single material point. If the stress contours are also themselves isoclines to the material point curves, that is an indication of steady-state flow. At 800°C, over a wide range of conditions, it seems that the stress contours are also isoclines. Also shown in Fig. 7 is the strain required for the onset of total sample recrystallization by grain boundary migration (after Rutter, 1995). It seems likely that the conditions for strain softening correspond with those for total dynamic recrystallization.

The recrystallized grain sizes produced in these

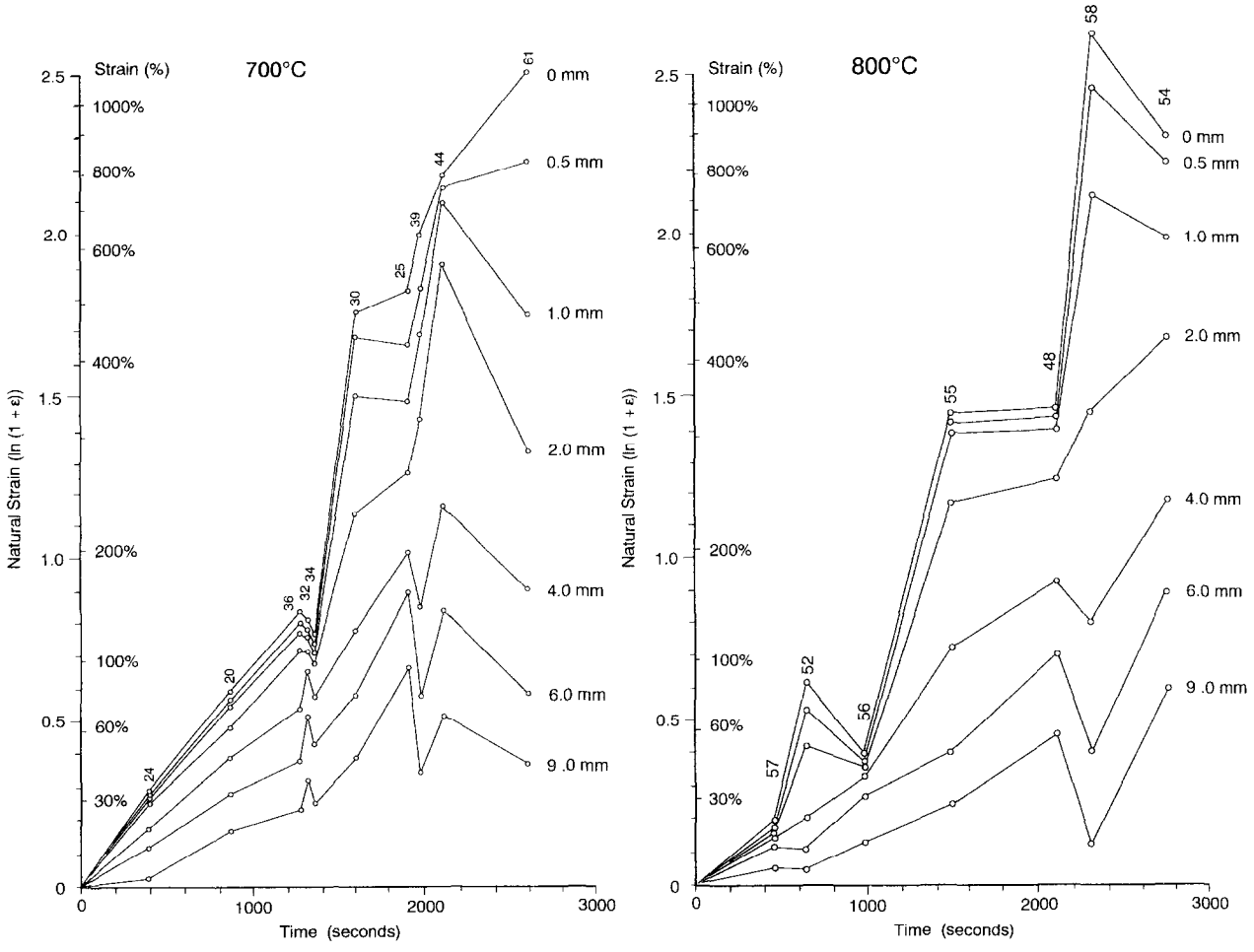

Fig. 6. Raw data from extension tests at 700°C and 800°C taken to different bulk stretch values. All tests were run at a constant displacement rate corresponding to an initial post-yield strain rate of $8 \times 10^{-4}\ s^{-1}$. Natural strain values and percentage conventional (extensional) strain are shown for material points along the specimens initially 0, 0.5, 1.9, 2.0, 4.0, 6.0 and 9.0 mm from the neck position, and linked by straight lines. Specimen number is shown at the top of each column of data. The deviations from smooth trends for each material point are attributable to a lack of reproducibility of behaviour, rather than to errors of measurement.

experiments are much too large to favour softening through change in deformation mechanism to grain size sensitive flow (Rutter, 1995). Softening may arise in this case from the mechanical recovery associated with removal of dislocation density during recrystallization (cf. quartz and feldspar behaviour during migration recrystallization (Tullis and Yund, 1985; Hirth and Tullis, 1992)). It is also apparent from thin-section observations that a strong crystallographic preferred orientation pattern is produced during dynamic migration recrystallization, that may additionally produce easy slip orientations (cf. Schmid *et al.*, 1987).

In Fig. 8, true constant strain rate stress–strain curves at 700°C and 800°C have been constructed from Fig. 6. At small strains, these curves are closely comparable to previously published data for Carrara marble (e.g. Schmid *et al.*, 1980), but there is a considerable stress drop at 800°C at large strains, apparently associated with dynamic recrystallization. At higher temperatures (e.g. 1000°C), total dynamic recrystallization develops at much smaller strains than at 800°C, almost immediately after yield (Rutter, 1995), and the lower flow stress probably reflects this. The flow stress at high strain at 800°C presumably therefore does not drop to a lower level than the small strain flow stress at 1000°C, and it seems reasonable to infer that the high strain flow stress that would ultimately develop at 800°C should be linked to the smaller strain flow stress at 1000°C for the purpose of describing the rheology. The Carrara marble rheology described by Schmid *et al.* (1980) shows a marked reduction in stress exponent, n, in the interval 800°C (at low strain rates) to 1000°C (at moderate strain rates). It is conceivable that this apparent rheology change is an expression of the microstructural changes that characterize deformation through this temperature interval, rather than representing a fundamental change in deformation mechanism.

Also shown in Fig. 8 are data of Schmid *et al.* (1987) from high strain direct shear tests at 800°C and 900°C, recast in terms of differential stress and shortening

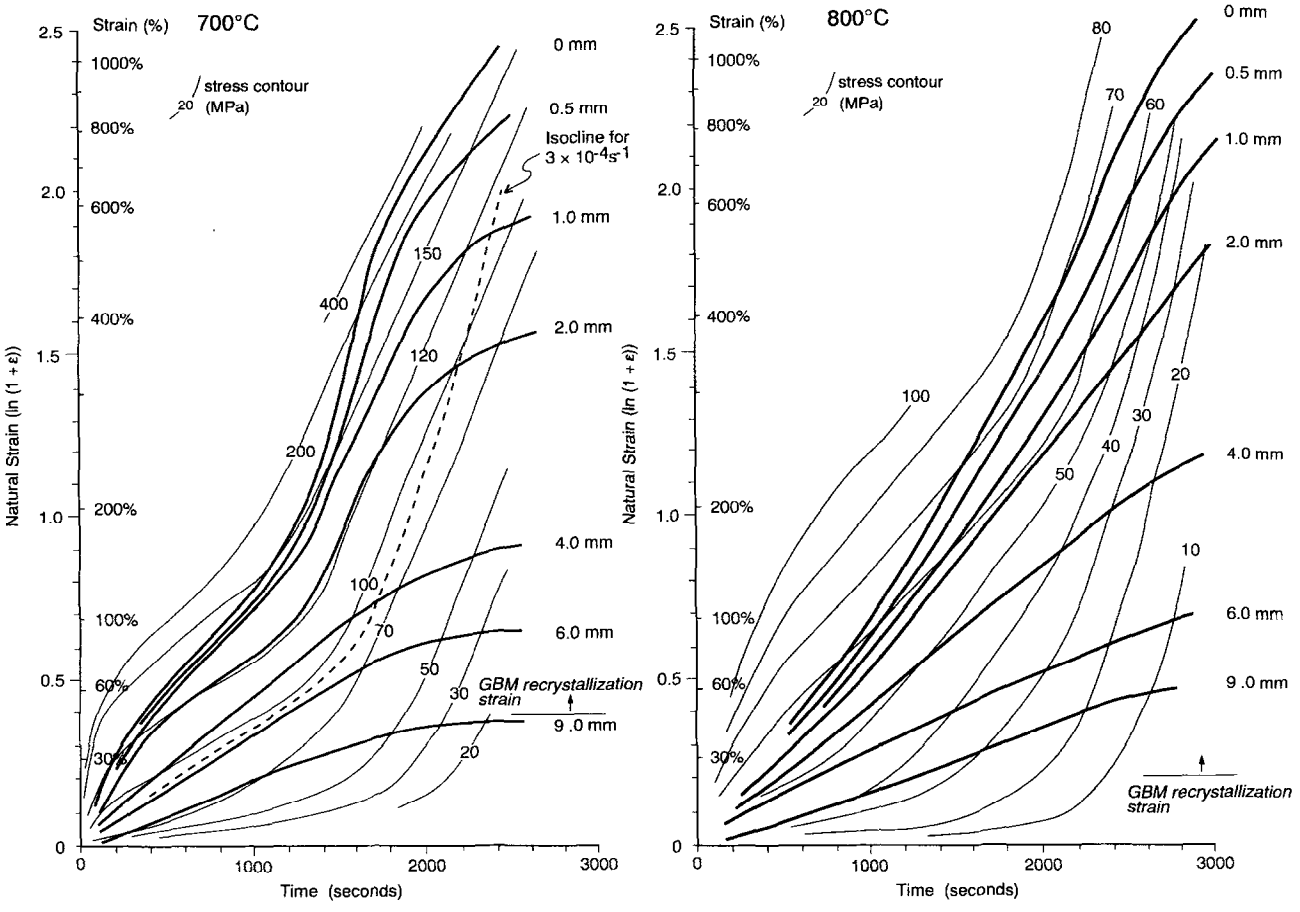

Fig. 7. Bold lines show smoothed curves corresponding to the line-linked data points shown in Fig. 6 at 700°C and 800°C. The local slope of these curves is the true strain rate at that point in the material. The plots are also contoured for differential stress values (MPa) computed from specimen shape and load supported at the end of each test. The strain required for the onset of total recrystallization by grain boundary migration (GBM) is also shown for each temperature (after Rutter, 1995). However, the high strain rate, necked regions of samples deformed at 700°C did not show complete GBM recrystallization, despite the high strains achieved. The acceleration of strain rate at the neck is apparent, especially at 700°C, and also the corresponding slowing of the deformation rate away from the neck. True constant strain rate trajectories can be constructed as isoclines to the strain–time curves. One for a constant strain rate of 3×10^{-4} s^{-1} (dashed curve) is shown at 700°C. The fact that this trends parallel to the stress contours implies steady state flow, but tending to strain hardening at high strains. At 800°C, the material point trajectories are themselves virtually isoclines. Over most of the high strain history beyond the onset of dynamic recrystallization, the isoclines unequivocally cut downwards through the stress contours to lower stress values, implying strain softening.

strain. These data show significant strain weakening at these temperatures. The low strain rate data from the extension tests at 800°C imply that strain weakening might be observed at low strains at both 800°C and 900°C. Accordingly, a number of true constant strain rate tests (displacement rate decreasing in correspondence with strain) were run in compression at 800°C and 900°C (note that in the more commonly reported constant displacement rate test, the true strain rate increases with total strain). Two such curves are shown in Fig. 8, and these clearly show strain weakening. This demonstrates the importance of running true constant strain rate tests at high temperatures when tests are run to large strains. The results of this study suggest that recrystallization-related strain weakening in relatively small strain tests on Carrara marble will only be seen over a narrow range of temperature and strain rate.

COMPARISON WITH METALS

Dynamic recrystallization is well known from studies on a number of metals. It tends to be favoured in metals with low stacking fault energy (e.g. copper), in which recovery by dislocation climb is inhibited through dislocation dissociation. It is much easier to produce large strain deformations in metals than in rocks, and both axisymmetric extension and shortening testing, and torsion testing have been employed. There is a sensitivity of behaviour to the type of test used (e.g. Weiss *et al.*, 1984) so that, for example, the large continuous strain gradients in solid bar torsion can lead to different recrystallized grain size characteristics compared to hollow tubular torsion.

Figure 9 summarizes the commonly reported phenomenology of dynamic recrystallization in metals (e.g. Sellars, 1978; Blaz *et al.*, 1983; Sakai, 1989). The

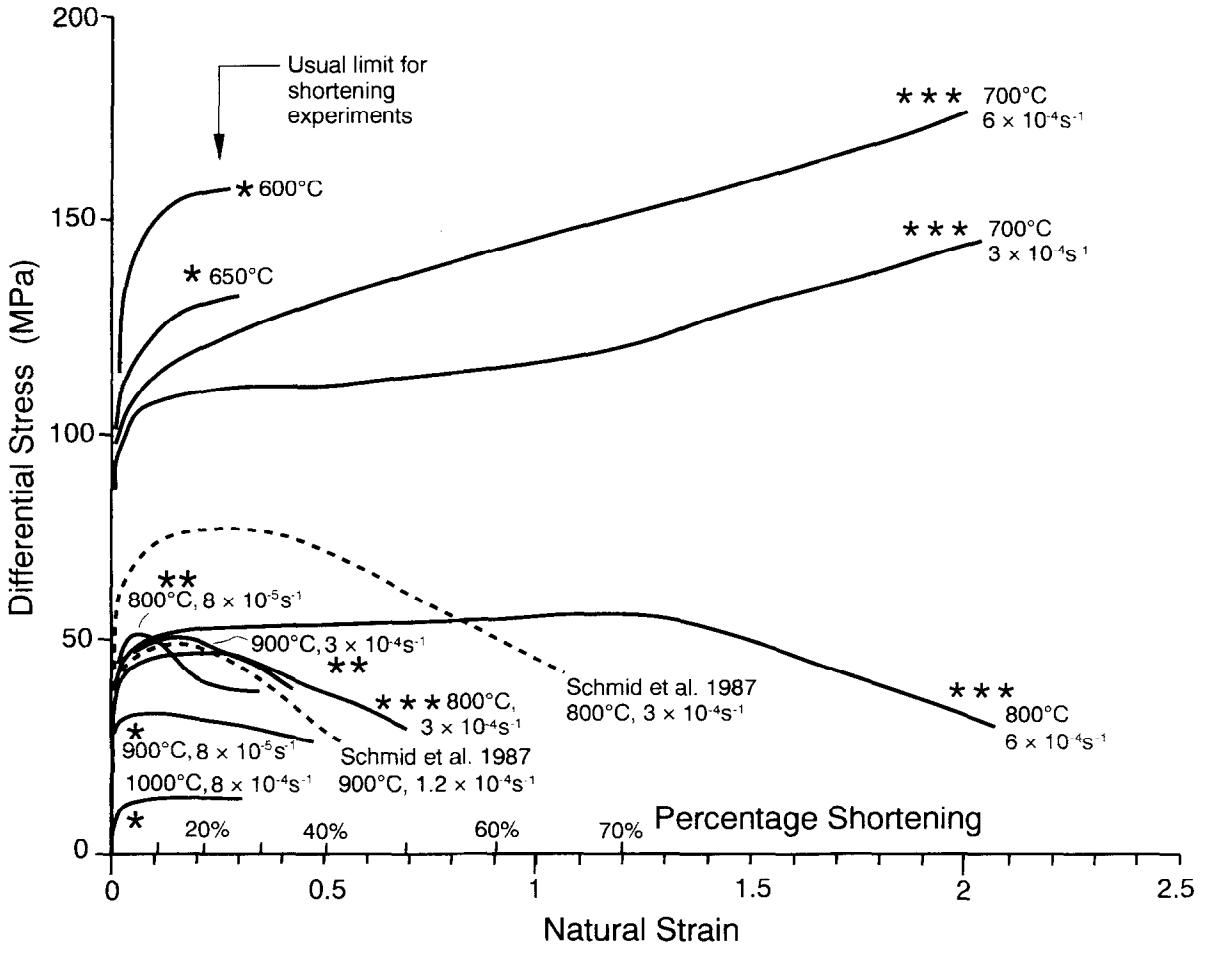

Fig. 8. High strain stress–strain curves for Carrara marble. Curves labelled '***' are constructed from Fig. 7. Curves labelled '**' are true constant strain rate compression tests. Those labelled '*' are conventional constant displacement rate compression tests. Dashed curves are direct shear test results of Schmid *et al.* (1987) recast in terms of differential stress and natural shortening strain. These clearly show strain weakening. The 700°C results imply strain hardening to high strains. At 800 and 900°C, there is clear strain weakening at high strains, under conditions of complete recrystallization by grain boundary migration. At 1000°C, recrystallization occurs immediately after yield so that strain weakening may not be apparent. For the strain weakening curves, it remains unclear as to what steady-state stress levels would eventually be attained.

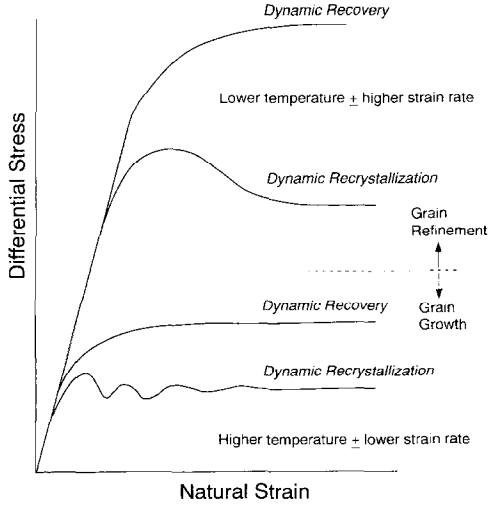

Fig. 9. Schematic summary of the high strain ($\varepsilon > 1$) hot-work behaviour of metals. Strain softening occurs when the strain required for recrystallization is less than that for steady flow by dynamic recovery. At high temperatures, multiple cycles of hardening and softening are seen, but only one at lower temperatures. The transition (marked by dashed line) appears to correspond also to the transition between grain refinement and grain growth of the recrystallized grains relative to the initial grain size (based on Sellars, 1978 and Sakai, 1989).

continual refreshment of the microstructure by grain boundary migration recrystallization is expected to result in a lower steady-state flow stress than by dynamic recovery. This will happen if the critical strain for recrystallization is attained before a steady-state microstructure for dynamic recovery creep. The wave of recrystallization and consequent weakening is expected to result in a strain softening characteristic. At combinations of high temperature and low strain rate (exemplified by a low value for the Zener–Holloman parameter, Z, or temperature-compensated strain rate, $Z = \dot{\varepsilon} \exp(H/RT)$, where H is the activation enthalpy for flow, R is the gas constant and T is the temperature in K), an immediately post-yield oscillation of the stress strain curve is seen. This corresponds to a series of recrystallization waves until eventually, a steady state is reached. Such an effect has not been seen for rocks. At high Z values, recrystallization results in a single stress peak. The transition between these behaviours corresponds approximately to the stress level below which, relative to the initial grain size, the dynamic recrystallization results in a grain size increase. As a result, the shape of the stress–strain curve

for dynamic recrystallization is sensitive to initial grain size (Blaz *et al.*, 1983). For Carrara marble, at the strain rates used in this study, this recrystallized grain size transition occurs at about 950°C. Below this temperature, we observe a single stress peak associated with dynamic recrystallization.

CONCLUSIONS

A series of extension tests have been carried out on Carrara marble to progressively higher bulk strains at 700°C and 800°C, in an attempt to determine whether strength changes accompany dynamic recrystallization of the whole specimen by grain boundary migration. The marked non-linearity of the strain rate sensitivity to stress for this material alone causes geometrical necking in extension, which disguises any strain-dependent variations in strength. Natural strains (ε) exceeding 2.4 ($> 1000\%$ extension) in the neck region can be produced. From the variation of finite strain and stress along the length of each specimen, isoclines of the strain–time curves for different material positions along the specimen allow synthesized constant strain rate stress–strain curves to be constructed.

At 700°C, steady state or slightly strain hardening flow occurs under most conditions, but at low strain rates at 800°C, clear strain softening occurs. The strain softening occurred in parallel with total dynamic recrystallization and moderate grain size reduction. Dynamic recrystallization may lead to weakening because the migration of grain boundaries sweeps deforming grains clear of dislocation density faster than recovery by dislocation climb. Texture development may also contribute to the observed weakening. These data imply that at 800°C or 900°C and at strain rates less than $10^{-4}\,s^{-1}$, strain softening might be seen in conventional compression tests up to strains of only 30%. From true constant strain rate tests in compression at these temperatures, this was confirmed to be correct. Similar observations were made by Schmid *et al.* (1987) from large strain direct shear (true constant strain rate) experiments on Carrara marble.

Dynamic recrystallization accompanied by a stress drop seems to be detectable in experiments only over a narrow range of temperature–strain rate conditions. In nature, the same behaviour will be seen at lower temperatures (perhaps around 300°C or above) at lower strain rates, and may favour localization of flow by intracrystalline plasticity when grain boundary migration recrystallized grain size is relatively large. At lower temperatures still, grain size reduction by subgrain rotation recrystallization may favour localization through a transition to grain-size-sensitive flow processes (Rutter, 1995).

An approximate value for the rate of change of flow stress with strain for this rock can be obtained from these experimental results, which may be useful for the numerical modelling of the necking phenomenon or the evolution of localized shear zones. However, the ultimate development of a steady state flow stress in the fully recrystallized material that showed a stress drop was never observed. At 1000°C, however, the rock recrystallized completely almost immediately after yield. The apparent stress–strain rate relations for Carrara marble may therefore be modified in this transitional behavioural regime.

Extensional testing of (suitable) rock types represents a useful way to study some aspects of mechanical behaviour and microstructural evolution at high strains. However, a degree of irreproducibility of specimen shape evolution detracts significantly from the utility of the method. Fluctuations in behaviour may arise from small differences in the thermal profile between different tests, or differences from test to test in the distribution of the first wave of recrystallization. The progressive evolution of sample shape must be very sensitive to the precise form of the profile developed in the elastic and immediately post-yield region. This methodology will complement other approaches to the study of high strain deformation of rocks.

Acknowledgements—This work was carried out with grant aid from the U.K. Natural Environment Research Council, ref. GR3/8627. Experimental Officer Robert Holloway provided invaluable assistance through equipment design, construction and maintenance, and Steve Covey-Crump is thanked for helpful discussions. Mervyn Paterson and an anonymous reviewer are thanked for helpful and constructive criticism.

REFERENCES

Blaz, L., Sakai, T. and Jonas, J. J. (1983) Effect of initial grain size on dynamic recrystallization of copper. *Metal Science* **17**, 609–616.

Carter, N. L. and Heard, H. C. (1970) Temperature and rate dependent deformation of halite. *American Journal of Science* **269**, 193–249.

Casey, M., Kunze, K. and Olgaard, D. (1998) Texture and microstructure for Solnhofen limestone deformed to high strains in torsion. *Journal of Structural Geology* **20**, 255–267.

Drury, M. R., Humphreys, F. J. and White, S. H. (1985) Large strain deformation studies using polycrystalline magnesium as a rock analogue. *Physics of the Earth and Planetary Interiors* **40**, 208–222.

Hart, E. W. (1967) Theory of the tensile test. *Acta Metallurgica* **15**, 351–355.

Heard, H. C. (1963) Effects of large changes in strain rate in the experimental deformation of Yule marble. *Journal of Geology* **71**, 162–195.

Heard, H. C. and Raleigh, C. B. (1972) Steady state flow in marble at 500–800°C. *Geological Society of America Bulletin* **83**, 935–956.

Hirth, G. and Tullis, J. (1992) Dislocation creep regimes in quartz aggregates. *Journal of Structural Geology* **14**, 145–159.

Hu, X. and Daehn, G. S. (1996) Effect of velocity on flow localization in tension. *Acta Materialia* **44**, 11021–11033.

Hutchinson, J. W. and Neale, K. W. (1977) Influence of strain rate sensitivity on necking under uniaxial tension. *Acta Metallurgica* **25**, 839–846.

Rutter, E. H. (1995) Experimental study of the influence of stress, temperature and strain on the dynamic recrystallization of marble. *Journal of Geophysical Research* **100**, 24651–24663.

Rutter, E. H., Casey, M. and Burlini, L. (1994) Preferred crystallographic orientation development during the plastic and superplastic flow of calcite rocks. *Journal of Structural Geology* **16**, 1431–1446.

Sakai, T. (1989) Dynamic recrystallization of metallic materials. In *Rheology of Solids and of the Earth*, eds S. Karato and M. Toriumi, pp. 284–307. Oxford University Press, Oxford.

Sellars, C. M. (1978) Recrystallization of metals during hot deforma-

tion. *Philosophical Transactions of the Royal Society of London* **A288**, 147–158.

Schmid, S. M., Boland, J. N. and Paterson, M. S. (1977) Superplastic flow in finegrained limestone. *Tectonophysics* **43**, 257–291.

Schmid, S. M., Panozzo, R. and Bauer, S. (1987) Simple shear experiments on calcite rocks: rheology and microfabric. *Journal of Structural Geology* **9**, 747–778.

Schmid, S. M., Paterson, M. S. and Boland, J. N. (1980) High temperature flow and dynamic recrystallization in Carrara Marble. *Tectonophysics* **65**, 245–280.

Tullis, J. and Yund, R. A. (1985) Dynamic recrystallization of feldspar: a mechanism for ductile shear zone formation. *Geology* **13**, 238–241.

Walker, A. N., Rutter, E. H. and Brodie, K. H. (1990) Experimental study of grain size sensitive flow of synthetic, hot-pressed calcite rocks. In *Deformation Mechanisms, Rheology and Tectonics*, eds R. J. Knipe and E. H. Rutter, pp. 259–284. Geological Society Special Publication **54**.

Weiss, I., Sakai, T. and Jonas, J. J. (1984) Effect of test method on transition from multiple to single peak dynamic recrystallization. *Metal Science* **18**, 77–84.